Check for updates

Original Research Article

Liposome Nanoparticles Carrying Oroxin A Regulate Epithelial-mesenchymal Transition and Induce Apoptosis in Hepatocellular Carcinoma Cells

Pharmacognosy Magazine
22(2) 552–564, 2026
© The Author(s) 2025
Article reuse guidelines:
in.sagepub.com/journals-permissions-india
DOI: 10.1177/09731296251348000
journals.sagepub.com/home/phm
Sage

Ru Gao[1] and Yuhang Guo[2]

Abstract

Background: PI3K/protein kinase B (AKT)/glycogen synthase kinase-3β (GSK-3β) regulates the activity of liver cancer cells. However, the poor water solubility of Oroxin A (OA) results in its lack of apparent clinical application effect, and liposome nanoparticles are relatively mature nanomaterials.
Objectives: This study aims to explore how liposome nanoparticles carry OA and regulate epithelial-mesenchymal transition (EMT) in liver cancer cells, providing a new theoretical basis and an experimental basis for nanomedicine treatment of liver cancer.
Materials and Methods: Prepare the OA-LN nano complex and use it in cell experiments to observe its anti-liver cancer effect and its effect on PI3K/AKT/GSK-3β to uncover the mechanism of its action on EMT. The efficacy of OA-LN was verified by an *in vivo* nude mouse experiment.
Results: OA-LN material was successfully prepared. OA-LN has a good tumor-suppressor effect in liver cancer. Intervening the PI3K/AKT/GSK-3β pathway can affect the activity of Bel-7402 cells to a certain extent and regulate their activity. The EMT was further verified using LY294002, 740Y-P, and Bel-7402. It was found that OA-LN can inhibit PI3K/AKT/GSK-3β signaling, thereby playing a certain inhibitory role in the EMT of Bel-7402 cells and further accelerating the apoptosis of Bel-7402 cells. *In vivo* experimental results showed that OA-LN had an obvious inhibitory effect on the weight and volume of tumor-bearing mice at the end of treatment, and the degree of cell necrosis was more obvious in hematoxylin and eosin (H&E) staining. It could significantly promote the apoptosis of tumor cells.
Conclusion: OA-LN is a potential new drug carrier for treating liver cancer. OA-LN has a unique ability to induce apoptosis in liver cancer cells. OA-LN can inhibit PI3K/AKT/GSK-3β signaling, thereby inhibiting the regulation of EMT and induction of apoptosis in liver cancer cells. It provides positive inspiration for developing targeted drugs and combined targeted therapy programs for liver cancer. It also has a certain referential significance for the treatment of other malignant tumors and provides a reasonable research basis for the treatment of malignant tumors.

Keywords

Liposome nanoparticles, Oroxin A, PI3K/AKT/GSK-3β, epithelial-mesenchymal transition, liver cancer

Received 25 September 2024; **revised** 22 January 2025; **accepted** 15 April 2025

Introduction

The incidence of liver cancer is higher in Asia (Li, Ramadori, et al., 2021). Due to the complex treatment methods and the severe side effects of therapeutic drugs, the cure rate is low and the cost of treatment is too high. Therefore, it is of great significance to study new methods for treating liver cancer.

Relevant studies have found that (Li, Zheng, et al., 2021) Oroxin A (OA) inhibits the proliferation and angiogenesis of tumor cells, induces apoptosis, and inhibits the development of inflammation. It has also been found to enhance the efficacy of radiotherapy and chemotherapy drugs and reduce their toxicity to normal cells (Guerrero et al., 2019). An animal experimental study found (Takada et al., 2023) that OA also has a significant inhibitory effect on lung and breast cancer growth in mouse models. The results show (Triana-Martínez et al., 2019) that OA may inhibit epithelial-mesenchymal transition (EMT) by affecting specific signaling pathways

[1]Department of Clinical Medicine, Tianjin Medical University, Tianjin, China
[2]Department of Oncology, Xi'an International Medical Center Hospital, Xi'an, Shaanxi, China

Corresponding author:
Yuhang Guo, Department of Oncology, Xi'an International Medical Center Hospital, Xi'an, Shaanxi 710100, China.
E-mail: 19054463522@163.com

Creative Commons Non Commercial CC BY-NC: This article is distributed under the terms of the Creative Commons Attribution-NonCommercial 4.0 License (http://www.creativecommons.org/licenses/by-nc/4.0/) which permits non-Commercial use, reproduction and distribution of the work without further permission provided the original work is attributed as specified on the SAGE and Open Access pages (https://us.sagepub.com/en-us/nam/open-access-at-sage).

such as Wnt and TGF-β, thereby reducing tumor invasion and metastasis. In addition, studies have also found (Wang et al., 2023) that OA may exert its anti-tumor effects through various mechanisms such as regulating the cell cycle, affecting cell signaling pathways, and regulating the expression of tumor-related genes. Although OA shows certain potential in tumor treatment, further clinical research is still needed to determine its efficacy and mechanism of action in liver cancer.

Studies have shown (Jin et al., 2019) that PI3K/protein kinase B (AKT)/glycogen synthase kinase-3β (GSK-3β) signaling is involved in the development and transformation of liver cancer, especially in the regulation of EMT. EMT consists of the transformation of cells from epithelial cells to mesenchymal cells. This cell biological transformation also affects tumor invasion, metastasis, and treatment resistance to a certain extent (Xu, Song, et al., 2021). PI3K/AKT/GSK-3β signaling can affect the activity of multiple transcription factors such as Snail, Slug, and Twist, promote the transformation of cells from epithelial cells to mesenchymal cells, change cell phenotypes, and enhance cell migration and invasion capabilities (Xu, Zhou, et al., 2021). In addition, activation of this signaling pathway may enable liver cancer cells to acquire stem cell properties and be more prone to EMT, thus increasing tumor invasion and metastasis capabilities. It can also promote the growth of tumors by regulating cell cycle-related proteins to promote cells to enter the proliferation phase (Hu et al., 2022). Although PI3K/AKT/GSK-3β signaling can regulate EMT and participate in the biological process of liver cancer cells, whether OA can regulate EMT in liver cancer through PI3K/AKT/GSK-3β signaling remains unclear.

OA is a bioactive ingredient, but it is difficult to absorb and utilize in the body, and its solubility is limited, which may affect its absorption and distribution in the body (Arab et al., 2021). Liposome nanoparticles can encapsulate OA in its internal lipid bilayer, which can enhance the bioavailability of the drug, improve its stability and biodistribution in the body, thereby increasing the efficacy of the drug and effectively improving the water solubility of the drugs and increasing the stability of drugs in the body (Ren et al., 2023). In addition, using liposome nanoparticles as drug carriers can encapsulate drugs inside them, reducing the direct contact between drugs and other components in the organism, thereby reducing toxic and side effects (Evers et al., 2022). Therefore, using liposome nanoparticles to carry OA cannot only improve the shortcomings of the drug but also further expand the use of OA in disease treatment, as well as the application of nanoliposomes in the medical field.

Materials and Methods

Experimental Materials

Liver cancer cell line Bel-7402 (Shanghai Hongshun Biotechnology); human normal liver cell line MG63 (Guangzhou Genio Biotech).

OA (purity: ≥98%, batch number: 57396-78-8, Shanghai Shidande) (see Figure 1); LY294002, 740Y-P (PI3K inhibitor, activator, purity: 99.95%, 96.35%, batch number: 154447-36-6, 1236188-16-1, Beijing Biolab); EMT-related protein monoclonal antibody (Shanghai Xinyu Biotech); PI3K, AKT, GSK-3β monoclonal antibody (Shanghai Yubo Biotechnology); secondary antibodies (Xi'an Baiying Biology).

Preparation and Characterization of Lignin A Carried by Liposome Nanoparticles

Preparation of liposome nanoparticles carrying OA materials precisely weighs appropriate amounts of OA, phospholipids, and hydroxypropyl-β-cyclodextrin. Place them in a flask, add a proper amount of absolute ethanol, and stir at a constant speed in a constant-temperature water bath. At the end of the reaction, after evaporating absolute ethanol, add chloroform for further reaction; dissolve, filter, wash, precipitate, combine, reduce pressure, recover, and dry to obtain dry OA-lipid nanoparticles, OA-LN.

Particle Size Distribution, Zeta Potential, and Morphology Analysis of OA-LN

After a small amount of OA-LN was diluted with distilled water, the particle size and zeta potential distribution were measured by a Zetasizer Nano-ZS potentiometer. After the suspension of OA-LN was diluted with ultra-pure water, the particle-size morphology of OA-LN was observed and photographed using transmission electron microscopy.

Analysis of Encapsulation Rate and Drug Loading of OA-LN

The nanoparticles and free drugs were separated by low-temperature and low-speed centrifugation. Then, 1 mL OA-LN solution was poured into a 10 mL volumetric bottle, and 9 mL

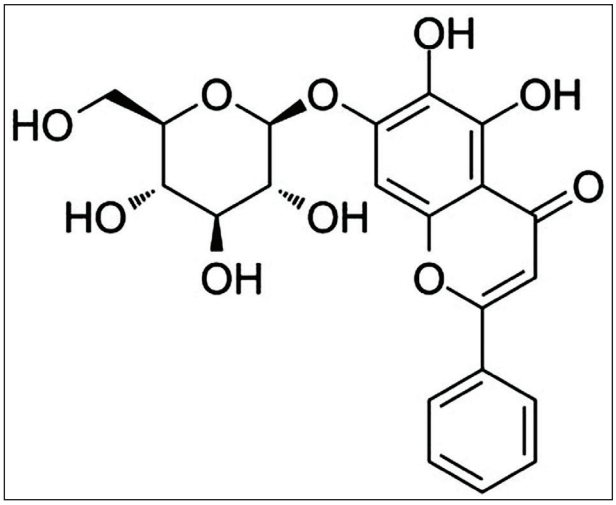


Figure 1. Molecular Structural Formula of Oroxin A (OA).

chromatograph-grade methanol was added for dilution. After mixing, OA-LN's encapsulation rate and drug loading were calculated according to the chromatographic conditions and standard curve equation.

Detection of OA-LN Release In Vitro

The release of OA-LN *in vitro* was analyzed using the dialysis bag method. 4 mL of OA-LN and OA were respectively placed in the dialysis bag and put in a shock water bath at 37°C, with the rotational speed set to 100 rpm. High-performance liquid chromatography (HPLC) detected the cumulative release of OA-LN for 24 h.

In Vitro Experiment

Cell Culture, Grouping, and Transfection

All cells were cultured using RPMI-1640 culture medium, and the operation process was strictly in accordance with the instructions. Cells were digested and passaged until the cell confluence reaches 80%. Bel-7402 cells were divided into a negative control group (NC group), an OA group (transfected with OA), an OA-LN group (transfected with OA-LN nanoparticles), an LY294002 group (transfected with PI3K inhibitor), and a 740Y-P group (transfected with PI3K activator).

The human normal liver cell line MG63 was used as the control group. The NC and the control groups were cultured with 50% phosphate-buffered saline (PBS) for 48 h for subsequent experimental operations.

Cell Proliferation

Cells were seeded into a 96-well plate (4×10^3 cells/well), cultured in a humidified incubator for 12 h, and treated in a humidified environment of 37°C and 5% CO_2 for 24 and 48 h. Then, discard the culture medium, add 10 μL 3-(4,5-dimethylthiazol-2-yl)-2,5-diphenyltetrazolium bromide (MTT) solution and 100 μL fresh Dulbecco's modified Eagle medium (DMEM), and continue culturing for 4 h. Place it on the floor with low-speed shaking for 10 min to dissolve it fully. A microplate reader measures the absorbance.

Cell Invasion

Place the treated cells in the upper Transwell chamber. Place the cells in the basement membrane matrix-precoated upper chamber. The cells in the upper chamber need to be inoculated in 15% fetal bovine serum (FBD), and the culture medium in the lower chamber must be used as a catalyst. Cultivate for 36 h at 37°C and 5% CO_2. Fixed with ethanol (20%), stained with crystal violet (0.2%), and photographed.

Apoptosis

After the cells in each group were digested, they were made into a suspension of 1×10^6 mL. After centrifugation and washing with PBS, they were resuspended. Buffer, Annexin V-FITC, and propidium iodide (PI) staining solution were added (measurements were 150, 10, and 5 μL) and incubated in the dark. After 15 groups, cell apoptosis was observed by flow cytometry.

Reverse Transcription-polymerase Chain Reaction (RT-PCR) Experiment

Logarithmically growing cells were harvested, reverse transcribed, and analyzed by RT-PCR. All mRNA expression values are presented relative to GAPDH, and relative expression levels were estimated using the $2^{-\Delta\Delta Ct}$ method. Table 1 lists the primers and their sequences.

Western Blotting

Logarithmically grown cells were harvested, digested, and protein concentrations were detected. Separate, transfer (10% SDS-PAGE), and incubate with a primary antibody at 4°C overnight. Wash and incubate the membrane with HRP-labeled secondary antibody for 1 h. Detection was enhanced by the internal reference glyceraldehyde-3-phosphate dehydrogenase (GAPDH).

Table 1. Real-time Polymerase Chain Reaction (PCR) Primers and Primer Sequences.

Primer		Sequences
PI3K	Forward primer	5′-GCTGGAGATGGTGTTGACTG-3′
	Reverse primer	5′-ACACTTCTGTGCAGGTGGAT-3′
AKT	Forward primer	5′-CTCTCGCTCCGCATTCCTTC-3′
	Reverse primer	5′-TGGAGGATGGTAGGGTGAGA-3′
GSK-3β	Forward primer	5′-TTTGGCCTTTGTGGAACATT-3′
	Reverse primer	5′-GAGGCTTGGATGCTCTTAGG-3′
GAPDH	Forward primer	5′-AAAGGGTCATCATCTCCGCC-3′
	Reverse primer	5′-AGTGATGGCATGGACTGTGG-3′

Note: AKT: Protein kinase B; GAPDH: Glyceraldehyde-3-phosphate dehydrogenase; GSK-3′: Glycogen synthase kinase-3′.

In Vivo Experiment

Construction of Liver Cancer Mouse Model

Bel-7402 cells with logarithmic growth were taken, centrifuged, and resuspended in RPMI-1640 medium, cultured to a concentration of 1.0×10^7/mL, and then inoculated into the subcutaneous skin of the right axillary of mice at a dose of 0.2 mL/cell under sterile conditions to establish a mouse model of transplanted liver cancer Bel-7402 cells. The hardness and volume of the tumor at the right axillary inoculation site of mice exceeded 100 mm^3, and the model was considered successful.

Group Intervention

Successful intervention modeling, mice were randomly divided into a normal saline group (NS), OA-LN group [OA-LN, 4 mg/(kg d)], and azithromycin group [ADM, 4 mg/(kg d)], with 6 mice in each group, injected three times a week. After 14 days of treatment, the peripheral venous blood of the mice were collected and killed. The tumor was excised and weighed. The tumor inhibition rate was calculated.

Serum Detection

The serum of mice in each group was collected, and the levels of TNF-α and IL-2 were detected by an enzyme-linked immunosorbent assay (ELISA) kit. The procedure should be carried out in strict accordance with the kit instructions, and the detection process should be repeated three times.

Tissue Detection

The tumor tissues of mice in each group were taken and fixed with paraformaldehyde (4%), the largest section was taken for the pathological section, and hematoxylin and eosin (H&E) staining was used at the same time, and the degree of necrosis of the tissues and tumor sections in each group was observed under the microscope. At the same time, the apoptosis of tumor cells was detected by terminal deoxynucleotidyl transferase dUTP nick-end labeling (TUNEL) analysis.

Statistical Analysis

All data were processed and analyzed using GraphPad Prism 8.0.2, and *F*-test was used, with $p < .05$ as the test standard.

Results

Through transmission electron microscopy, OA-LN was observed to be uniformly spherical (Figure 2A) with a particle size <200 nm (Figure 2B), and the potential distribution was 11.69 mV (Figure 2C), suggesting that the nanomaterials were stable. The encapsulation rate of OA-LN was 96.30% ± 1.32%, and the drug loading was 12.65% ± 0.89%. At the same time, as shown in Figure 2D, the cumulative release degree of OA-LN in 24 h is about 80%. In comparison, OA is released completely within 24 h, and the cumulative drug release rate reaches 100%, indicating that OA-LN has good slow-release performance.

OA-LN has a Good Tumor-suppressor Effect in Liver Cancer

We found through cell experimental culture that with the extension of intervention time, the proliferation of liver cancer under OA-LN intervention was inhibited (Figure 3A vs. other groups, $p < .05$), and the intervention weakened the invasive ability of Bel-7402 cells (Figure 3B vs. other groups, $p < .05$). The apoptosis rate of the OA-LN group also confirmed this phenomenon (Figure 3C vs. other groups, $p < .05$); during this period, we found that OA has a positive tumor-suppressor effect in liver cancer, and OA-LN is the most prominent.

The Activity and EMT Ability of Liver Cancer Cells are Related to the Expression Level of PI3K/AKT/GSK-3β

We then detected the levels of PI3K, AKT, and GSK-3β in MG63 cells and Bel-7402 cells, respectively, and found that their levels were significantly increased in the Bel-7402 cells (Figure 4A vs. control group, $p < .05$). At the same time, we used LY294002 and 740Y-P to intervene in Bel-7402 cells, respectively, in further research. The intervention of cells with LY294002 can effectively reduce the expression of PI3K, accompanied by a decrease of AKT and GSK-3β expression. In contrast, the expression levels of PI3K, AKT, and GSK-3β in cells in the 740Y-P group showed an opposite trend (Figure 4A vs. other groups, $p < .05$), indicating that LY294002 and 740Y-P affected the PI3K/AKT/GSK-3β pathway intervention was successful. Further analysis of the activity of Bel-7402 cells found that the proliferation ability of the LY294002 group was significantly inhibited (Figure 4B vs. other groups, $p < .05$). The above experiments reflect that downregulating the expression of the MEK/ERK pathway is beneficial in inhibiting the progression of liver cancer. At the same time, it was observed that, in the LY294002 group, N-cadherin and vimentin expression in Bel-7402 cells were significantly reduced. In contrast, E-cadherin expression was increased (Figure 4C vs. other groups, $p < .05$), indicating that it was found that interfering with the expression of the PI3K/AKT/GSK-3β pathway can effectively affect the EMT of liver cancer cells.

PI3K/AKT/GSK-3β Signaling Involves in the Process of OA-LN Inhibiting Liver Cancer Activity

In order to further explore the mechanism of A-LN inhibiting liver cancer activity, based on OA-LN intervention, we used 740Y-P and LY294002 to intervene in Bel-7402 cells, respectively. We found that the inhibition of Bel-7402 cell

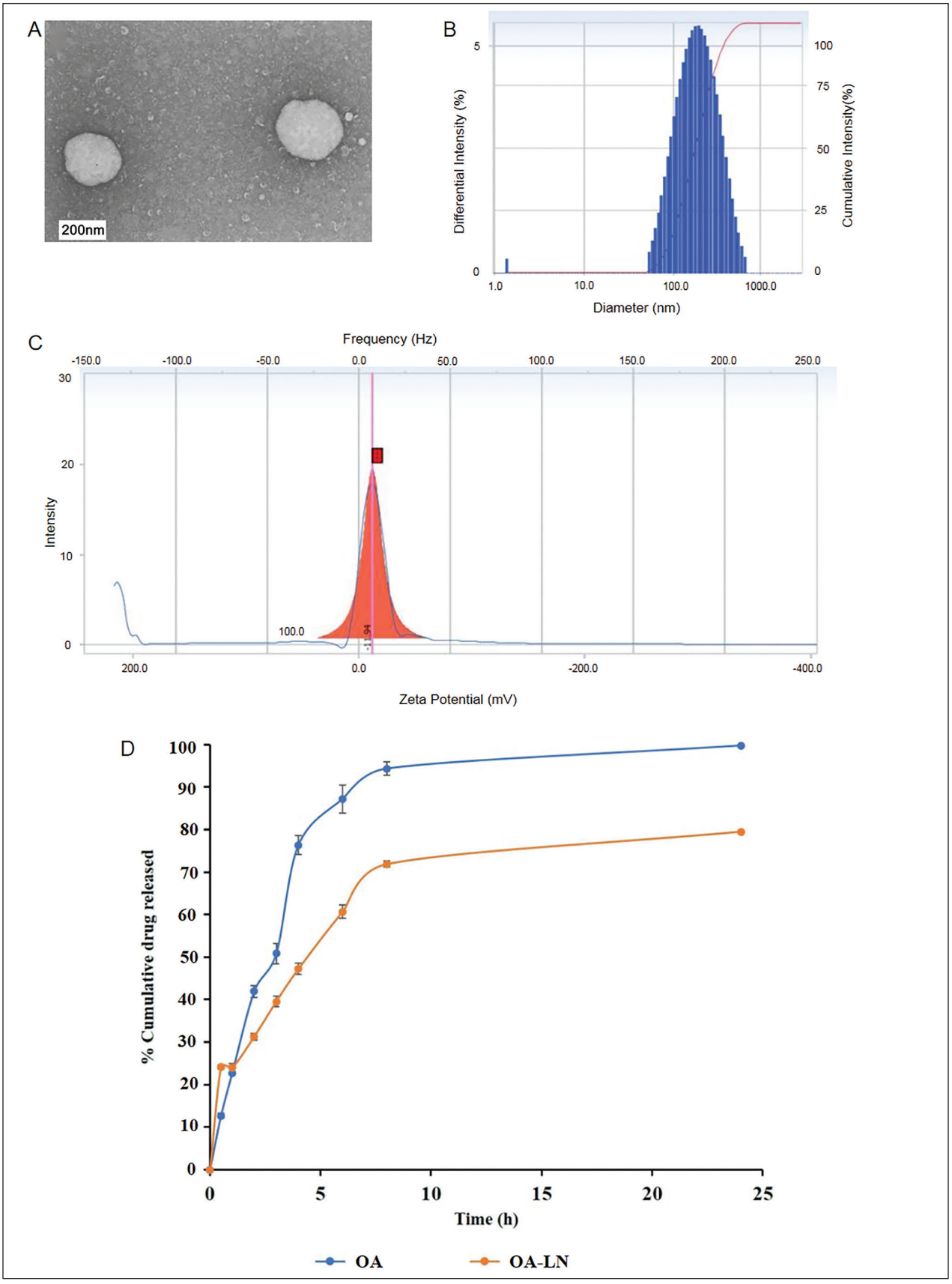


Figure 2. Structural Characterization of OA-LN.

Note: (A) Transmission electron microscope image of OA-LN, 200 nm; (B) Size diagram of OA-LN nanoparticles; (C) Zeta potentiogram of OA-LN nanoparticles; (D) Release curve of OA-LN *in vitro*.

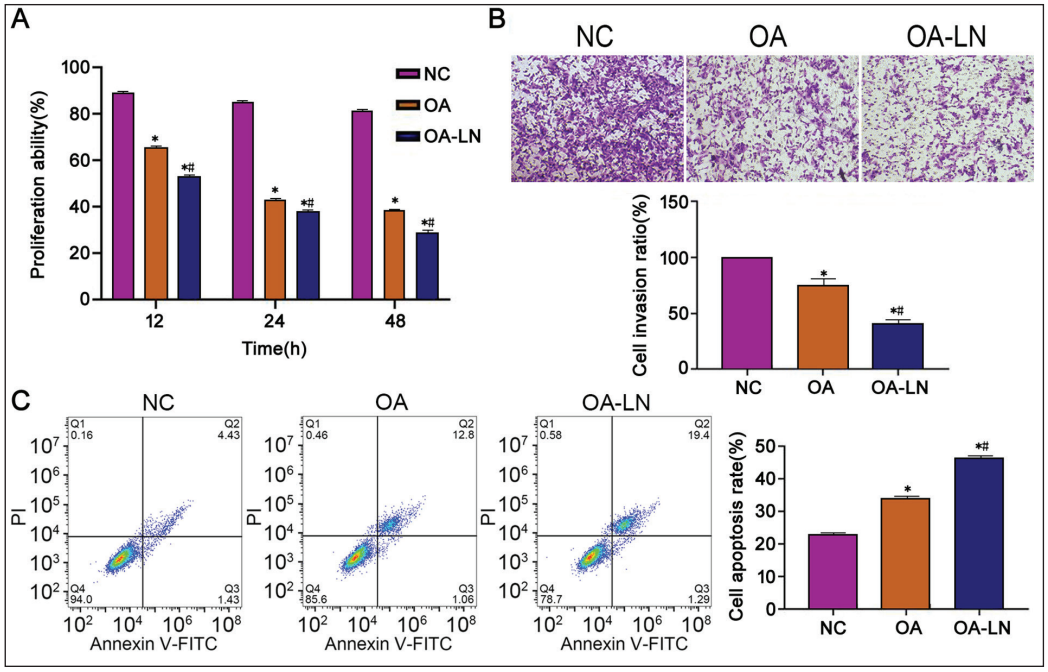


Figure 3. OA-LN has a Good Tumor-suppressor Effect in Liver Cancer (n = 6).

Note: (A) 3-(4,5-Dimethylthiazol-2-yl)-2,5-diphenyltetrazolium bromide (MTT) detects the proliferation ability of Bel-7402 cells; (B) Transwell chamber detects the invasion of Bel-7402 cells and the histogram shows the invasion ability; (C) Flow cytometry detects the apoptosis of Bel-7402 cells, the histogram shows apoptotic ability. Compared with negative control (NC) group, *p < .05; compared with Oroxin A (OA) group, #p < .05.

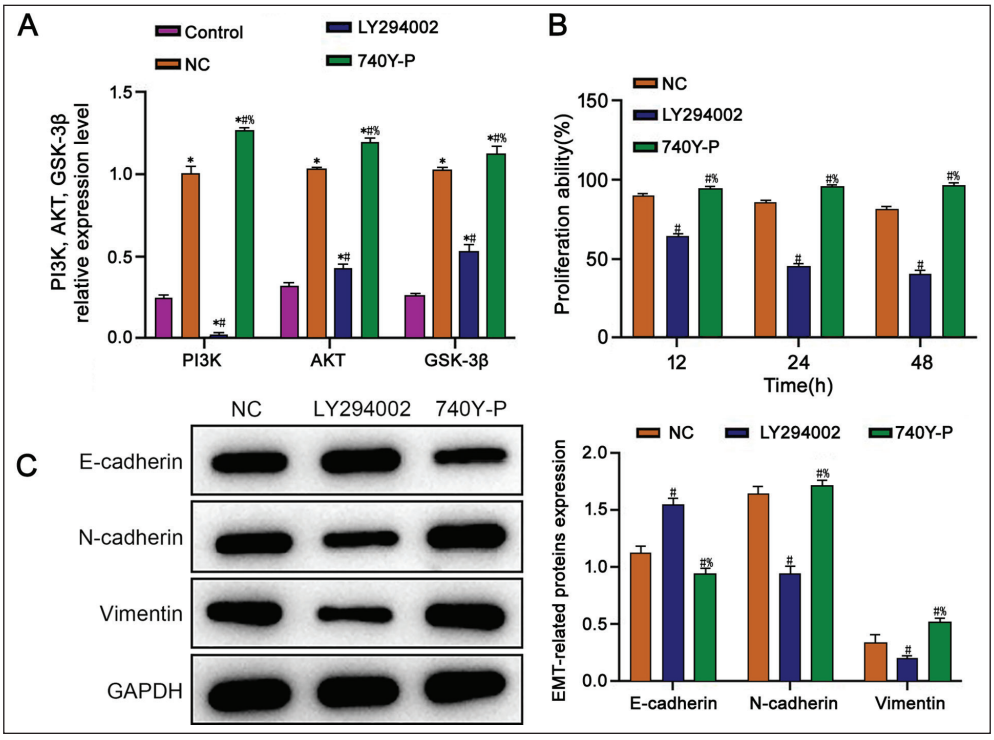


Figure 4. The PI3K/Protein Kinase B (AKT)/Glycogen Synthase Kinase-3β (GSK-3β) Signaling Pathway can Regulate the Epithelial-mesenchymal Transition (EMT) of Liver Cancer Cells (n = 6).

Notes: (A) Reverse transcription-polymerase chain reaction (RT-PCR) experiment detects the expression of PI3K, AKT, and GSK-3β mRNA in Bel-7402 cells; (B) 3-(4,5-dimethylthiazol-2-yl)-2,5-diphenyltetrazolium bromide (MTT) detects the proliferation ability of Bel-7402 cells; (C) Expression of epithelial-mesenchymal transition proteins. Compared with the control group, *p < .05; compared with the negative control (NC) group, #p < .05; compared with the LY294002 group, %p < .05.

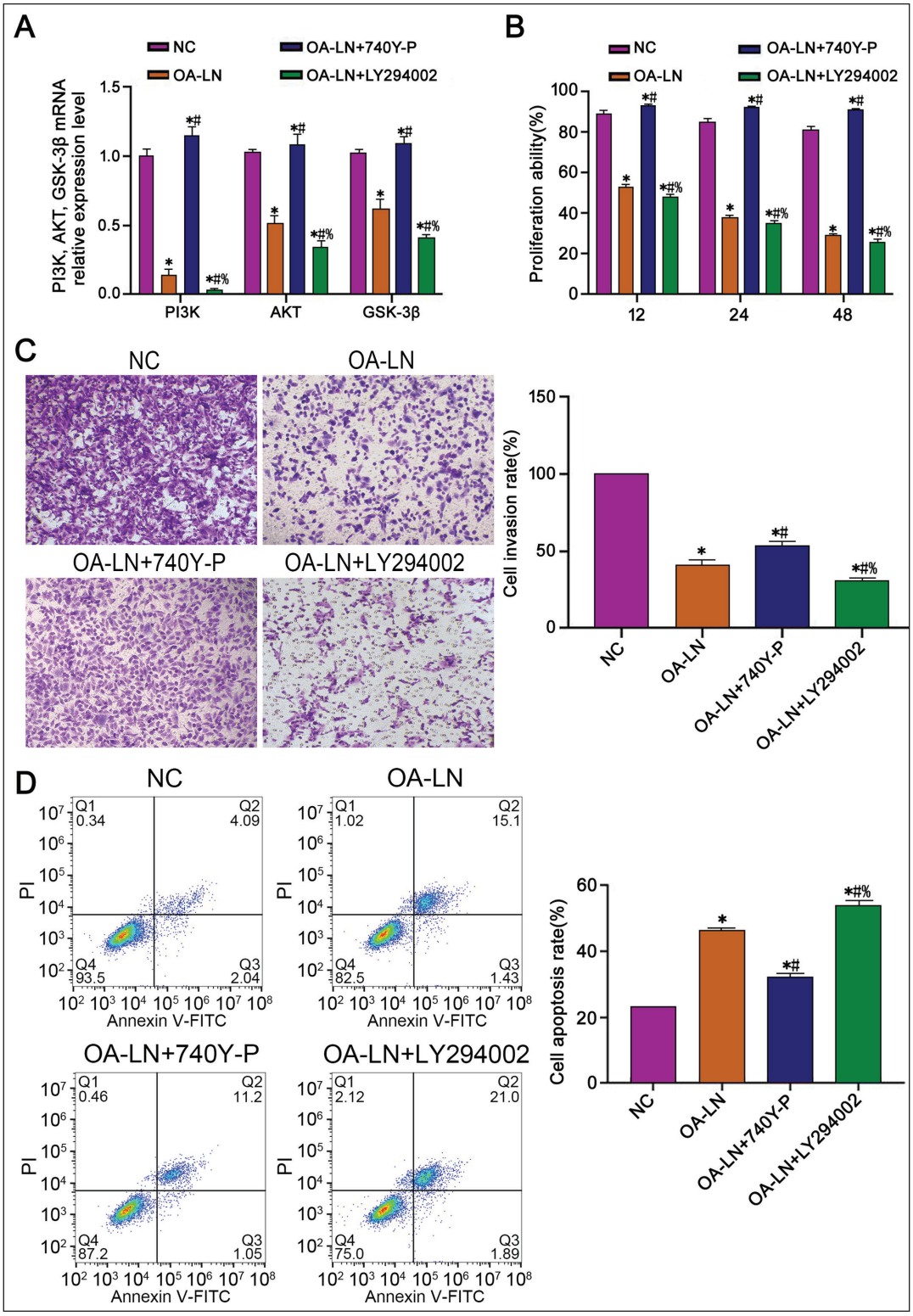


Figure 5. The PI3K/Protein Kinase B (AKT)/Glycogen Synthase Kinase-3β (GSK-3β) Signaling Pathway is Involved in the Inhibitory Activity of OA-LN on Liver Cancer (n = 6).

Notes: (A) Reverse transcription-polymerase chain reaction (RT-PCR) experiment detects the expression of PI3K, AKT and GSK-3β mRNA in Bel-7402 cells; (B) 3-(4,5-dimethylthiazol-2-yl)-2,5-diphenyltetrazolium bromide (MTT) detects the proliferation ability of Bel-7402 cells; (C) Transwell chamber detects Bel-7402 cell invasion, square The figure shows the invasion ability, 100 μm; (D) Flow cytometry detects the apoptosis of Bel-7402 cells and the histogram shows the apoptosis ability. Compared with negative control (NC) group, *p < .05; compared with OA-LN group, #p < .05; compared with OA-LN + 740Y-P group, %p < .05.

proliferation and invasion was amplified by LY294002 (Figure 5B–5C vs. other groups, $p < .05$). At the same time, the ability of apoptosis increased significantly (Figure 5D vs. other groups, $p < .05$), indicating that LY294002 played a key role under OA-LN intervention. In the following experimental process, we mainly observed the specific role of LY294002 in this process. Through protein experiments, we found that PI3K, AKT, and GSK-3β mRNA levels in Bel-7402 cells treated with OA-LN were significantly reduced (Figure 5A vs. NC group, $p < .05$), indicating that OA-LN can inhibit the PI3K/AKT/GSK-3β pathway. At the same time, we added LY294002 to the OA-LN group and showed more significantly decreased PI3K, AKT, and GSK-3β (Figure 5A vs. other groups, $p < .05$), indicating that PI3K/AKT/GSK-3β is downregulated.

OA-LN can Promote Cell Apoptosis by Inhibiting EMT of Liver Cancer Cells via PI3K/AKT/GSK-3β Signaling

In order to verify the above experiment, we added 740Y-P on the basis of OA-LN + LY294002 intervention and found that the PI3K, AKT, and GSK-3β protein levels of Bel-7402 cells were reversed (Figure 6A vs. other groups, $p < .05$). When we further clarified the inhibitory mechanism of OA-LN on liver cancer, we found that the N-cadherin and vimentin

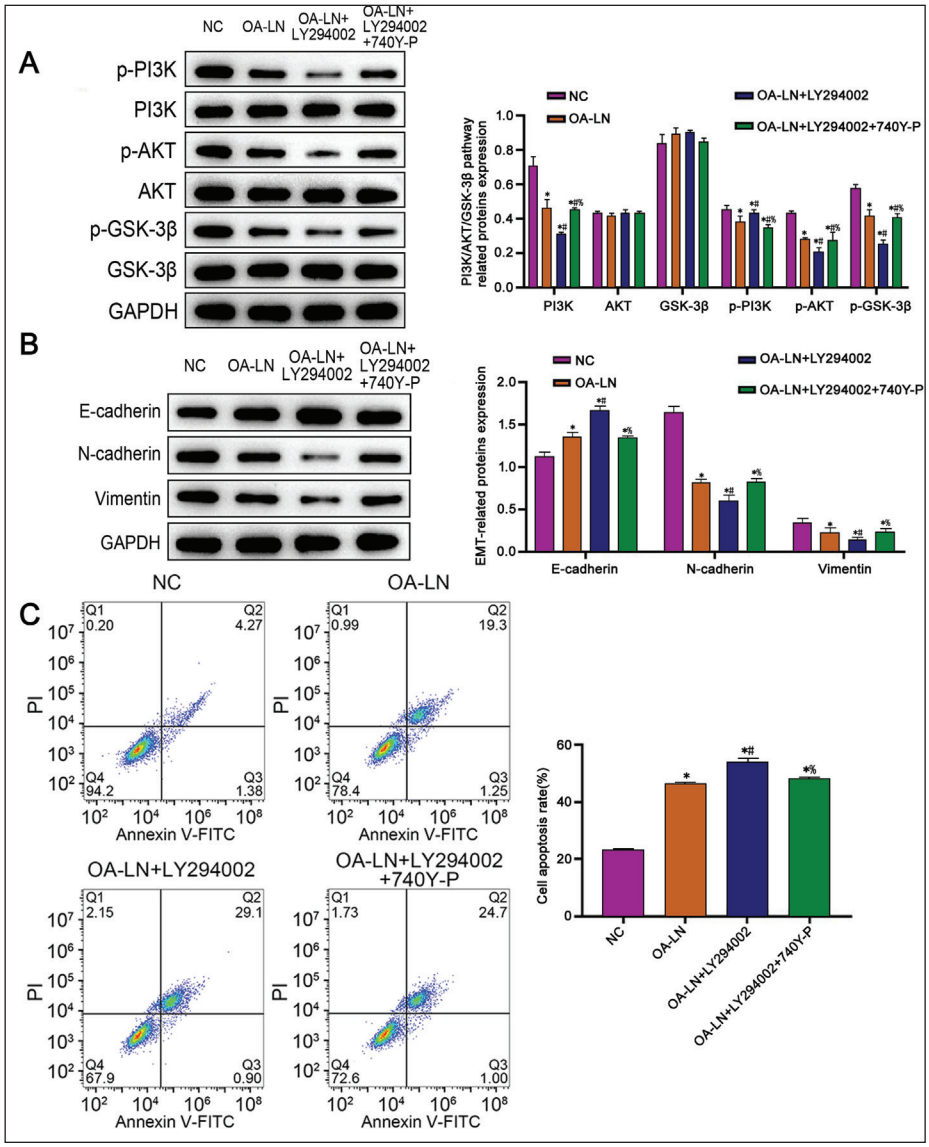


Figure 6. OA-LN can Inhibit the Epithelial-mesenchymal Transition (EMT) of Liver Cancer Cells by Inhibiting the PI3K/Protein Kinase B (AKT)/Glycogen Synthase Kinase-3β (GSK-3β) Signaling Pathway, Thereby Promoting Cell Apoptosis ($n = 6$).

Notes: (A) Western blotting detects the expression of proteins related to the PI3K/AKT/GSK-3β signaling pathway; (B) Western blotting detects the expression of proteins related to epithelial-mesenchymal transition; (C) Flow cytometry detects the apoptosis of Bel-7402 cells. Histogram showing apoptotic capacity. Compared with negative control (NC) group, *$p < .05$; compared with OA-LN group, #$p < .05$; compared with OA-LN + LY294002 group, %$p < .05$.

expression in Bel-7402 cells in the OA-LN group were significantly reduced, while the expression of E-cadherin protein showed an opposite trend (Figure 6Bvs. NC group, $p < .05$), and after adding LY294002, the changes in N-cadherin, vimentin, and E-cadherin protein levels in Bel-7402 cells were more obvious (Figure 6B vs. other groups, $p < .05$). At the same time, we added 740Y-P to the OA-LN + LY294002 group, and the results showed that the above-mentioned protein levels in Bel-7402 cells were reversed (Figure 6B vs. OA-LN + LY294002 group, $p < .05$), which was further verified. OA-LN downregulated PI3K/AKT/GSK-3β and inhibited the EMT of liver cancer cells.

At the same time, further observation showed a decreased apoptotic ability of Bel-7402 cells in the OA-LN + LY294002 + 740Y-P group (Figure 6C vs. OA-LN + LY294002 group, $p < .05$), indicating that OA-LN promotes apoptosis of liver cancer cells by inhibiting the EMT of liver cancer cells in the process of downregulating the PI3K/AKT/GSK-3β pathway.

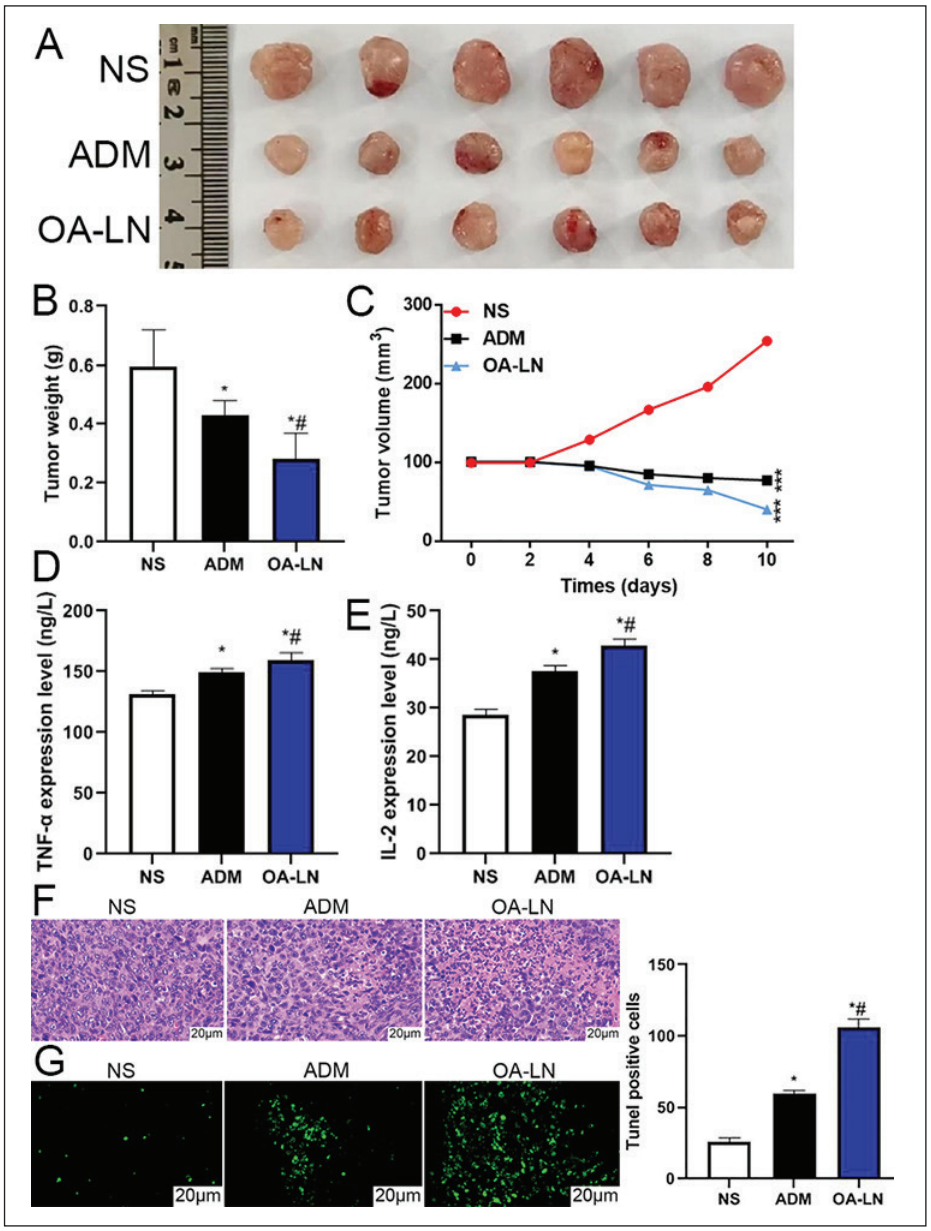


Figure 7. Results of OA-LN Treatment in Hepatocellular Carcinoma Bearing Mice ($n = 6$).

Notes: (A) Tumor *in vitro* map of each group; (B) Tumor weight of each group after treatment; (C) Tumor growth curves of each group of mice; (D) Serum TNF-α was detected by enzyme-linked immunosorbent assay (ELISA); (E) Serum IL-2 levels were detected by ELISA; (F) The histopathological changes of tumor in each group were observed by hematoxylin and eosin (H&E) staining (100 μm); (G) Apoptosis of tumor cells in each group was detected by terminal deoxynucleotidyl transferase dUTP nick-end labeling (TUNEL) (25 μm). Compared with the normal saline (NS) group, *$p < .05$; compared with azithromycin group (ADM) group, #$p < .05$.

The Therapeutic Effect of OA-LN in Hepatocellular Carcinoma was Verified by Animal Experiments

In order to further verify the therapeutic effect of OA-LN in liver cancer, this study constructed nude mice with liver cancer tumors with Bel-7402 cells, and the modeling success rate was 100%. After the intervention of model mice with OA-LN and ADM at the same time, it was found that the tumor weight and tumor volume of mice in the two groups were significantly reduced compared with that in the NS group (vs. NS group, $p < .05$) and OA-LN had a more significant effect on the weight and volume of mice at the end of treatment (vs. ADM group, $p < .05$), as shown in Figure 7A–7C.

At the same time, it was observed that the serum levels of TNF-α and IL-2 in the OA-LN group and ADM group were significantly higher than those in the NS group ($p < .05$), and the improvement was more obvious in the OA-LN group (vs. ADM group, $p < .05$), as shown in Figure 7D–7E. H&E staining was further used to observe the pathological changes in the mice in each group. As can be seen from Figure 7F, tumor cells in the NS group were in a good growth state, with deep nuclear staining and few necrotic cells. However, there were fewer tumor cells in the ADM group and OA-LN group, with a loose intercellular arrangement and different degrees of necrosis that could be seen, and the degree of necrosis of cells in the OA-LN group was more obvious, indicating that OA-LN had anti-tumor effects. At the same time, by TUNEL staining, it was found that the ADM group and OA-LN group had stronger green fluorescence, and the OA-LN group had stronger fluorescence intensity (Figure 7G), indicating that OA-LN could effectively promote apoptosis.

Discussion

Studies have reported (Arab et al., 2021; Shang et al., 2019) that OA can promote β-catenin phosphorylation by regulating GSK-3β activity, thereby accelerating the degradation of β-catenin and inhibiting it to a certain extent. The occurrence of EMT, thus, exerts an anti-cancer effect. In addition, OA can interfere with the cycle progression of pancreatic cancer cells by blocking the degradation of IκB, preventing the nuclear translocation of NF-κB, reducing phosphatidylinositol (3,4,5)-trisphosphate (PIP3), and inhibiting GSK-3β activity, ultimately mediating the reduction of MMPs and Cyclin D1 (Fang et al., 2019; Qu et al., 2022). However, the solubility of OA in water is low, and it is easily degraded and metabolized by plasma enzymes, gastric acid, and others in the body, resulting in insufficient efficacy (Gade et al., 2022; Xu, Jiang, et al., 2021). Therefore, we use liposome nanoparticles to encapsulate OA inside them, which cannot only effectively prevent its degradation and metabolism and improve the stability of the drug, but also reduce the toxicity and side effects of OA on normal tissues. In addition, liposome nanoparticles carrying OA can aggregate in tumor tissues more effectively, increase the drug concentration of OA in tumor cells, and reduce damage to normal cells (Katoch et al., 2020). Therefore, we successfully prepared OA-LN composite materials. To prove that OA-LN has a good inhibitory effect, we found through cell experiments that, under the intervention of OA, cell proliferation and invasion abilities were significantly reduced, and the apoptosis rate was greatly increased. The OA-LN group showed more consistent results. Therefore, it shows that OA-LN has a good tumor-suppressor effect in liver cancer.

Studies have found (Chen et al., 2021; Wu et al., 2022) that in diabetes and neurodegenerative diseases, the PI3K/AKT pathway inhibitor LY294002 can inhibit PI3K activation, thereby reducing AKT activation and inhibiting colorectal cancer (CRC) cell proliferation. At the same time, GSK-3β, as a multifunctional kinase, can play a certain role in the process of glycogen metabolism. According to relevant studies, the PI3K/AKT signaling pathway can regulate EMT by targeting the expression of its downstream gene GSK-3β, and phosphorylating the Snail transcription factor (Navaei et al., 2021). In addition, Kao et al. (2014) found in their study that by regulating the regulatory level of GSK-3β/Snail/E-cadherin, EMT can be effectively regulated, thus playing a regulatory role in the invasion and metastasis of lung cancer cells. Therefore, it can be considered that the downstream PI3K/AKT gene GSK-3β can regulate EMT through phosphorylation of the Snail transcription factor, thus participating in the occurrence and development of tumors. We used LY294002 and 740Y-P to conduct experiments and found that under the intervention of LY294002, the cell proliferation ability was greatly reduced within a certain time, E-cadherin increased, and N-cadherin and vimentin showed opposite changes. However, after adding 740Y-P, the changing trend of protein expression was also reversed. Therefore, it shows that inhibiting the PI3K/AKT/GSK-3β signaling pathway can affect the activity of liver cancer cells and regulate the EMT of liver cancer cells. Using PI3K inhibitors inhibits the activity of PI3K, thereby preventing the occurrence of PI3K phosphorylation, leading to reduced activity of the PI3K/AKT signaling pathway and, to a certain extent, reducing the activity of tumor cells and enhancing their therapeutic effect. In addition, by inhibiting AKT activity, mTOR activation and GSK-3β phosphorylation can be reduced, thereby reducing protein synthesis and cell growth of cancer cells. At the same time, inhibiting AKT and FOXO can be maintained in the nucleus, thereby increasing the expression of p27Kip1 and inhibiting CDK activity, thereby inhibiting the proliferation and survival of cancer cells. LY294002 also protects neurons from the induction of apoptosis and improves symptoms of neurodegenerative diseases.

To explore whether PI3K/AKT/GSK-3β signaling is involved in the inhibitory activity of OA-LN on liver cancer, the combined intervention of OA-LN, 740Y-P, and LY294002 showed that the ability of the OA-LN + LY294002 group to

inhibit liver cancer activity was stronger than that of OA-LN alone. The reason may be that LY294002 inhibits PI3K activation and weakens the occurrence of AKT phosphorylation to a certain extent. The inhibitory ability of OA-LN against liver cancer is enhanced. OA-LN +7 40Y-P was in a weaker state because 740Y-P activated PI3K/AKT signaling and promoted the phosphorylation of AKT, thus weakening the inhibitory effect of OA-LN on liver cancer. This also suggests that the PI3K/AKT/GSK-3β pathway is involved in the process of OA-LN inhibiting liver cancer activity. In addition, related studies have found (Gai et al., 2019; Lin et al., 2020) that downregulating PLDA2 can inhibit the PI3K/AKT/MTR pathway, increase GSK-3β phosphorylation, and affect MMPs and cyclin D1 expression, and at the same time, it also reduces the expression of EMT-related genes such as Snail and Slug, ultimately promoting autophagy, thereby clearing damaged organelles, reducing cellular stress levels, and inhibiting the EMT process. In addition, inhibiting GSK-3β activity will cause NF-κB to enter the nucleus and promote the transcription of MMPs, thereby enhancing their expression and activity and disrupting epithelial-cell-mesenchymal junctions (Nath et al., 2022; Tsai et al., 2021). We added 740Y-P to the intervention of OA-LN + LY294002 and found that 740Y-P reversed the effect of OA-LN + LY294002 on inhibiting EMT and promoting cell apoptosis in liver cancer cells. However, current research still requires further research on the safe dose of OA-LN.

At the same time, after the successful preparation of OA-LN, due to the enhanced permeability and retention (EPR) effect *in vivo*, OA-LN can more easily enter the cells so as to achieve the therapeutic effect on tumors. In this study, the tumor-bearing mouse model of liver cancer was further constructed to observe the tumor inhibitory effect in the animals. The results showed that OA-LN intervention could significantly inhibit the growth of liver cancer and induce the apoptosis of tumor cells. This indicates that OA-LN has a high application value *in vivo*. At the same time, further observation showed that the levels of TNF-α and IL-2 in the serum of mice showed an obvious upward trend after OA-LN intervention. Among them, TNF-α is the strongest tumor-inhibiting cytokine, which has no obvious effect on normal cells but has an obvious direct killing effect on tumor cells and can inhibit the proliferation of anti-tumor cells to a certain extent. At the same time, IL-2 also plays an important role in the body's immune regulation. It can promote the expression level of T cells and B cells in the body and then induce them to secrete more cytokines, thus playing a role in killing tumor cells and inhibiting tumor angiogenesis. In this study, after the intervention of OA-LN, the levels of TNF-α and IL-2 in mice were increased, which indicates that OA-LN can affect the immune regulatory function of the body during the treatment of liver cancer. Previous studies have found that in the process of inhibiting cell proliferation and invasion of non-small cell lung cancer, the E-cadherin level is significantly increased, and IL-2 expression is significantly promoted (Loh et al., 2019). This indicates that OA-LN can inhibit both EMT and immune escape during the treatment of liver cancer, but this specific mechanism still needs to be further explored.

Conclusion

In summary, OA-LN can inhibit the PI3K/AKT/GSK-3β signaling, thereby inhibiting and regulating EMT and inducing apoptosis of liver cancer cells. As a new drug carrier for treating liver cancer, OA-LN provides positive inspiration for the development of liver cancer-targeted drugs and combined targeted therapy programs. It also has a certain referential significance for the treatment of other malignant tumors and provides good guidance for the treatment of malignant tumors.

However, this study also has some shortcomings. For example, OA-LN has not been applied in clinical practice in this study, and the long-term therapeutic effect and safety of OA-LN for patients cannot be clarified. At the same time, this study is still in the basic experimental stage, and the mechanism pathway involved in the study has not been analyzed in detail. In addition, there are many mechanisms by which PI3K/AKT/GSK-3β affects epithelial-mesenchymal transformation, which has not been deeply explored in this study, which is also the limitation of this study. In future research, we need to explore further and verify the mechanism of these problems.

Abbreviations

AKT: Protein kinase B; DMEM: Dulbecco's modified Eagle medium; EMT: Epithelial-mesenchymal transition; GAPDH: Glyceraldehyde-3-phosphate dehydrogenase; GSK-3β: Glycogen synthase kinase-3β; LN: Liposome nanoparticles; MTT: 3-(4,5-Dimethylthiazol-2-yl)-2,5-diphenyltetrazolium bromide; OA: Oroxin A; PI3K: Phosphoinositide-3 kinase; RT-PCR: Reverse transcription-polymerase chain reaction.

Acknowledgments

The authors gratefully acknowledge the Xi'an International Medical Center Hospital for providing the necessary equipment for this study.

Declaration of Conflicting Interests

The authors declared no potential conflicts of interest with respect to the research, authorship, and/or publication of this article.

Ethical Approval and Informed Consent

This study was approved by the Ethics Committee of Xi'an International Medical Center Hospital.

Funding

The authors received no financial support for the research, authorship, and/or publication of this article.

ORCID iD

Yuhang Guo https://orcid.org/0009-0005-2989-3513

References

Arab, H. H., Safar, M. M., & Shahin, N. N. (2021). Targeting ROS-dependent AKT/GSK-3beta/NF-kappaB and DJ-1/Nrf2 pathways by dapagliflozin attenuates neuronal injury and motor dysfunction in rotenone-induced Parkinson's disease rat model. *ACS Chemical Neuroscience*, *12*(4), 689–703. https://doi.org/10.1021/acschemneuro.0c00722

Chen, W., Xian, G., Gu, M., Pan, B., Wu, X., Ye, Y., Zheng, L., Zhang, Z., & Sheng, P. (2021). Autophagy inhibitors 3-MA and LY294002 repress osteoclastogenesis and titanium particle-stimulated osteolysis. *Biomaterials Science*, *9*(14), 4922–4935. https://doi.org/10.1039/d1bm00691f

Evers, M. J. W., van de Wakker, S.I., de Groot, E. M., de Jong, O. G., Gitz-François, J. J. J., Seinen, C. S., Sluijter, J. P. G., Schiffelers, R. M., & Vader, P. (2022). Functional siRNA delivery by extracellular vesicle-liposome hybrid nanoparticles. *Advanced Healthcare Materials*, *11*(5), Article e2101202. https://doi.org/10.1002/adhm.202101202

Fang, C., Jiang, B., Shi, X., & Fan, C. (2019). Hes3 enhances the malignant phenotype of lung cancer through upregulating cyclin D1, cyclin D3 and MMP7 expression. *International Journal of Medical Sciences*, *16*(3), 470–476. https://doi.org/10.7150/ijms.28139

Gade, I. S., Chadeneau, C., Tagne Simo, R., Atchade, A. T., Talla, E., Seite, P., Vannier, B., Guillard, J., Laurent, S., Henoumont, C., Nwabo Kamdje, A. H., & Muller, J.-M. (2022). A new flavonoid glycoside from *Tapinanthus* sp. (Loranthaceae) and evaluation of anticancer activity of extract and some isolated compounds. *Natural Product Research*, *36*(16), 4085–4093. https://doi.org/10.1080/14786419.2021.1963243

Gai, X., Tang, B., Liu, F., Wu, Y., Wang, F., Jing, Y., Huang, F., Jin, D., Wang, L., & Zhang, H. (2019). mTOR/miR-145-regulated exosomal GOLM1 promotes hepatocellular carcinoma through augmented GSK-3β/MMPs. *Journal of Genetics and Genomics*, *46*(5), 235–245. https://doi.org/10.1016/j.jgg.2019.03.013

Guerrero, A., Herranz, N., Sun, B., Wagner, V., Gallage, S., Guiho, R., Wolter, K., Pombo, J., Irvine, E. E., Innes, A. J., Birch, J., Glegola, J., Manshaei, S., Heide, D., Dharmalingam, G., Harbig, J., Olona, A., Behmoaras, J., Dauch, D., … Gil, J. (2019). Cardiac glycosides are broad-spectrum senolytics. *Nature Metabolism*, *1*(11), 1074–1088. https://doi.org/10.1038/s42255-019-0122-z

Hu, X., Zou, M., Ni, L., Zhang, M., Zheng, W., Liu, B., & Cheng, Z. (2022). Dec1 deficiency ameliorates pulmonary fibrosis through the PI3K/AKT/GSK-3β/β-catenin integrated signaling pathway. *Frontiers in Pharmacology*, *13*, Article 829673. https://doi.org/10.3389/fphar.2022.829673

Jin, F., Wu, Z., Hu, X., Zhang, J., Gao, Z., Han, X., Qin, J., Li, C., & Wang, Y. (2019). The PI3K/Akt/GSK-3beta/ROS/eIF2B pathway promotes breast cancer growth and metastasis via suppression of NK cell cytotoxicity and tumor cell susceptibility. *Cancer Biology and Medicine*, *16*(1), 38–54. https://doi.org/10.20892/j.issn.2095-3941.2018.0253

Kao, S. H., Wang, W. L., Chen, C. Y., Chang, Y. L., Wu, Y. Y., Wang, Y. T., Wang, S. P., Nesvizhskii, A. I., Chen, Y. J., Hong, T. M., & Yang, P. C. (2014). GSK3β controls epithelial-mesenchymal transition and tumor metastasis by CHIP-mediated degradation of Slug. *Oncogene*, *33*(24), 3172–3182. https://doi.org/10.1038/onc.2013.279

Katoch, D., Kumar, D., Padwad, Y. S., Singh, B., & Sharma, U. (2020). Narciclasine-4-*O*-beta-D-xylopyranoside, a new narciclasine glycoside from *Zephyranthes minuta*. *Natural Product Research*, *34*(2), 233–240. https://doi.org/10.1080/14786419.2018.1527836

Li, X., Ramadori, P., Pfister, D., Seehawer, M., Zender, L., & Heikenwalder, M. (2021). The immunological and metabolic landscape in primary and metastatic liver cancer. *Nature Reviews Cancer*, *21*(9), 541–557. https://doi.org/10.1038/s41568-021-00383-9

Li, X., Zheng, J., Chen, S., Meng, F.-D., Ning, J., & Sun, S.-L. (2021). Oleandrin, a cardiac glycoside, induces immunogenic cell death via the PERK/elF2alpha/ATF4/CHOP pathway in breast cancer. *Cell Death and Disease*, *12*(4), 314. https://doi.org/10.1038/s41419-021-03605-y

Lin, J., Song, T., Li, C., & Mao, W. (2020). GSK-3beta in DNA repair, apoptosis and resistance of chemotherapy, radiotherapy of cancer. *Biochimica et Biophysica Acta—Molecular Cell Research*, *1867*(5), Article 118659. https://doi.org/10.1016/j.bbamcr.2020.118659

Loh, C.-Y., Chai, J. Y., Tang, T. F., Wong, W. F., Sethi, G., Shanmugam, M. K., Chong, P. P., & Looi, C. Y. (2019). The E-cadherin and N-cadherin switch in epithelial-to-mesenchymal transition: Signaling, therapeutic implications and challenges. *Cells*, *8*(10), Article 1118. https://doi.org/10.3390/cells8101118

Nath, N., Rana, A., Nagini, S., & Mishra, R. (2022). Glycogen synthase kinase-3beta inactivation promotes cervical cancer progression, invasion and drug resistance. *Biotechnology and Applied Biochemistry*, *69*(5), 1929–1941. https://doi.org/10.1002/bab.2258

Navaei, Z. N., Khalili-Tanha, G., Zangouei, A. S., Abbaszadegan, M. R., & Moghbeli, M. (2021). PI3K/AKT signaling pathway as a critical regulator of cisplatin response in tumor cells. *Oncology Research*, *29*(4), 235–250. https://doi.org/10.32604/or.2022.025323

Qu, L., Tian, Y., Wang, F., & Li, Z. (2022). NOVA1 promotes NSCLC proliferation and invasion by activating Wnt/beta-catenin signaling. *BMC Cancer*, *22*(1), 1091. https://doi.org/10.1186/s12885-022-10164-8

Ren, Y., Kaweesa, E. N., Tian, L., Wu, S., Sydara, K., Xayvue, M., Moore, C. E., Soejarto, D. D., Cheng, X., Yu, J., Burdette, J. E., & Kinghorn, A. D. (2023). The cytotoxic cardiac glycoside (-)-cryptanoside A from the stems of *Cryptolepis dubia* and its molecular targets. *Journal of Natural Products*, *86*(6), 1411–1419. https://doi.org/10.1021/acs.jnatprod.3c00094

Shang, L., Pin, L., Zhu, S., Zhong, X., Zhang, Y., Shun, M., Liu, Y., & Hou, M. (2019). Plantamajoside attenuates isoproterenol-induced cardiac hypertrophy associated with the HDAC2 and AKT/GSK-3beta signaling pathway. *Chemico-Biological Interactions*, *307*, 21–28. https://doi.org/10.1016/j.cbi.2019.04.024

Takada, Y., Kaneko, K., & Kawakami, Y. (2023). Interaction of odoroside A, A known natural cardiac glycoside, with Na^+/K^+-ATPase. *The Journal of Membrane Biology*, *256*(3), 229–241. https://doi.org/10.1007/s00232-023-00281-1

Triana-Martínez, F., Picallos-Rabina, P., Da Silva-Álvarez, S., Pietrocola, F., Llanos, S., Rodilla, V., Soprano, E., Pedrosa, P.,

Ferreirós, A., Barradas, M., Hernández-González, F., Lalinde, M., Prats, N., Bernadó, C., González, P., Gómez, M., Ikonomopoulou, M. P., Fernández-Marcos, P. J., García-Caballero, T., … Collado, M. (2019). Identification and characterization of cardiac glycosides as senolytic compounds. *Nature Communications*, *10*(1), 4731. https://doi.org/10.1038/s41467-019-12888-x

Tsai, C.-L., Jung, S.-M., Chi, L.-M., Tsai, C.-N., Lin, C.-Y., Chao, A., & Lee, Y.-S. (2021). Glycogen synthase kinase-3 beta (GSK3beta)-mediated phosphorylation of ETS1 promotes progression of ovarian carcinoma. *Aging*, *13*(10), 13739–13763. https://doi.org/10.18632/aging.202966

Wang, J., Sun, J., Jin, L., Wang, M., Huang, Y., Jin, M., Zhou, W., & Li, G. (2023). A new monoterpenoid glycoside and a new phenolic glycoside isolated from *Dracocephalum moldavica* and their anti-complementary activity. *Natural Product Research*, *37*(2), 169–179. https://doi.org/10.1080/14786419.2021.1957885

Wu, X., Pu, L., Chen, W., Zhao, Q., Wu, G., Li, D., & Zhu, H. (2022). LY294002 attenuates inflammatory response in endotoxin-induced uveitis by downregulating JAK3 and inactivating the PI3K/Akt signaling. *Immunopharmacology and Immunotoxicology*, *44*(4), 510–518. https://doi.org/10.1080/08923973.2022.2055565

Xu, Y., Jiang, X., Xu, J., Qu, W., Xie, Z., Jiang, R.-W., & Feng, F. (2021). A previously undescribed phenylethanoid glycoside from *Callicarpa kwangtungensis* Chun acts as an agonist of the Na/K-ATPase signal transduction pathway. *Phytochemistry*, *181*, Article 112577. https://doi.org/10.1016/j.phytochem.2020.112577

Xu, H., Song, D., Xu, R., & He, X. (2021). BAFF signaling drives interstitial transformation of mouse renal tubular epithelial cells in a Pin1-dependent manner. *In Vitro Cellular & Developmental Biology Animal*, *57*(6), 649–659. https://doi.org/10.1007/s11626-021-00598-y

Xu, S., Zhou, Y., Biekemitoufu, H., Wang, H., Li, C., Zhang, W., & Ma, Y. (2021). Expression of Twist, Slug and Snail in esophageal squamous cell carcinoma and their prognostic significance. *Oncology Letters*, *21*(3), 184. https://doi.org/10.3892/ol.2021.12445